Available online at www.sciencedirect.com
ScienceDirect
LWT 40 (2007) 1018–1026
LWT
www.elsevier.com/locate/lwt

Characterization of sol–gel transitions of food hydrocolloids with near infra-red spectroscopy

Yiqun Huang[a], Anna G. Cavinato[b], Juming Tang[c,*], Barry G. Swanson[d], Mengshi Lin[d], Barbara A. Rasco[d]

[a]Department of Family, Nutrition, and Exercise Sciences, Queens College, The City University of New York, Flushing, NY 11367-1597, USA
[b]Chemistry Program, Eastern Oregon University, One University Blvd., La Grande, OR 97850, USA
[c]Department of Biological Systems Engineering, Box 646120, Washington State University, Pullman, WA 99164-6120, USA
[d]Department of Food Science and Human Nutrition, Box 646376, Washington State University, Pullman, WA 99164-6376, USA

Received 19 January 2006; received in revised form 30 June 2006; accepted 7 July 2006

Abstract

Near infra-red spectroscopy (NIR, 600–1100 nm) was used to characterize sol–gel transitions of food hydrocolloids including whey protein (WP), high acyl (HA) and low acyl (LA) gellan gums. Whey protein (20% w/w), LA and HA gellan (1% w/v) aqueous solutions with selected calcium concentrations (0–40 mM) were used. Principal components analysis (PCA) and principal component regression (PCR) were performed to analyze spectral data of gel dispersions at a series of controlled temperatures (20–95 °C). Gelling temperatures of gellan dispersions were determined directly based upon the PCA results without requiring for reference values. The gelling temperatures determined with the NIR method were similar to those obtained by dynamic rheological tests and dielectric property test. The PCR models showed a good predictability for temperatures of gellan dispersions with selected calcium concentrations during cooling or heating process. This study indicates that the NIR method has a great potential to detect structural change, and to monitor time and temperature dependant behaviour of food hydrocolloids during sol–gel transition period.

Keywords: Near infra-red; Sol–gel transition; Food hydrocolloid; Gellan; Whey protein

1. Introduction

Sol–gel transitions of food hydrocolloids are important topics from both fundamental and technological points of views. Sol–gel transition mechanism decides the gel properties of a food gum including, but not limiting to structural stability as well as rheological properties. Various technologies have been applied to study sol–gel transitions of food hydrocolloids, including rheometry, differential scanning calorimetry (DSC), electron spin resonance (ESR), nuclear magnetic resonance (NMR), dielectric property test, and spectroscopic methods. While the sensitivity and/or application scope of DSC and dielectric property test are questionable, NMR and ESR are complicated and prohibitively costly. Rheological testing is the most widely used method for the characterization of biopolymers. For a general rheological test regarding sol–gel transition mechanism of a biopolymer system, an external force is applied to the biopolymer system and the amplitude of the deformation or the force of resistance to the deformation is measured at each time period or temperature range. The test is normally based upon the assumption that when a new external force is applied, the previous external force would no longer have any effect on the molecular structure of the hydrocolloid system, which may not be possible since the deformed structure of a visco-elastic material may need a long time to completely recover if it is recoverable.

Near infra-red spectroscopy (NIR) has provided solutions to many agricultural and pharmaceutical problems as a rapid and nondestructive method over the past two decades. NIR detects the absorption or reflection intensity

*Corresponding author. Tel.: +1 509 335 2140; fax: +1 509 335 2722.
E-mail addresses: yiqun.huang@qc.cuny.edu (Y. Huang), jtang@wsu.edu (J. Tang).

0023-6438/$30.00
doi:10.1016/j.lwt.2006.07.005

of a light incident (700–2500 nm) on a material. The reflectance or transmittance rate is ultimately determined by the chemical and physical properties of the tested material. NIR spectra are mainly composed of overtone and combination bands due to hydrogen stretching vibrations. Although the complex nature of NIR spectra requires data interpretation through mathematical and statistical approaches, NIR methods have a great potential for nondestructive analysis of a sample with minimal or no prior sample preparation.

NIR spectroscopy has been used to characterize food hydrocolloid systems. Lundin, Stenlöf and Hermansson (1998) determined storage modulus (G′, 0–3500 Pa) of mixtures of carrageenan, locust bean gum and casein with NIR spectroscopy. A correlation coefficient of 0.85 and a root mean square (RMS) error of prediction of 540 Pa were obtained. A study by Segtnan, Kvaal, Rukke, Schüller, and Isaksson (2003) showed the possibility of using NIR to determine bloom value, viscosity, pH and moisture content of gelatine. Thygesen, Engelsen, Madsen, and Sorensen (2001) predicted viscosity behaviour of potato starch with NIR method. Bao, Cai and Corke (2001) determined gelatinization onset, peak temperatures and textural properties of rice starch with NIR methods and indicated that NIR analysis was sufficiently accurate for routine screening of a large number of samples. Closs, Conde-Petit, Roberts, Tolstoguzov, and Escher (1999) employed NIR to determine phase separation kinetics of aqueous starch-galactomannan system and revealed reasonable results. Castillo, Payne, Hicks, Laencina, and Lopéz (2003) studied casein aggregation with NIR method and found out that milk coagulation involved aggregation and curd firming stages separately. Although the physico-chemical properties of biopolymer aqueous solutions may have no direct relationship with their NIR spectra, these physico-chemical properties may be highly correlated with their chemical properties (such as composition and molecular structure) that have a direct correlation with NIR spectra. Therefore, a correlation or mathematical model between physico-chemical properties and NIR spectra of these biopolymer solutions can be established that enable to predict (or determine) the unknown physico-chemical properties of other solutions based on their spectra data.

Whey protein is normally defined as milk proteins soluble at pH 4.6 and 20 °C (Bottomley, Evans, & Parkinson, 1990). The major components of whey protein are α-lactalbumin and β-lactoglobulin. Under an appropriate condition, whey protein solutions form gels on heating through protein denaturation. The gelling temperature varies depending on the composition and concentration of whey protein solutions.

Gellan gum is a linear anionic polysaccharide gelling agent consisting of tetrasaccharide repeating units. Gellan is commercially available in two forms: low acyl (LA) and high acyl (HA) gellan powder. HA gellan has side chains, L-glycerate and acetate groups at its glucose residues while LA gellan does not. The structural difference between LA and HA gellan leads to a disparity of rheological and textural properties between these two polymers. LA gellan solutions have relatively low gelling temperatures and form strong and firm gels; while HA gellan solutions have high gelling temperatures and form soft and week gels. Unlike whey protein, gellan solutions with appropriate concentrations form gels upon cooling. Addition of cations such as calcium normally accelerates the gelation process of gellan solutions.

The objective of this study was to explore the use of NIR to characterize the sol–gel transitions of whey protein, LA and HA gellan aqueous solutions. The specific focuses included the determination of gelling temperatures, the detection of structural changes as well as the characterization of time and temperature-dependant behaviour during heating or cooling process.

2. Materials and methods

2.1. Sample preparation

Both LA (Kelcogel F) and HA (Kelcogel LT100) gellan polymers were provided by CP Kelco US, Inc. (Wilmington, DE, USA). Whey protein concentrate (Alacen 882) was provided by NZMP, Inc. (Santa Rosa, CA, USA). Gellan dispersions (1% w/v) with selected calcium concentrations (0–40 mM) and whey protein dispersions (20% w/w) were used for the study.

To prepare for 1% gellan dispersions, one gram of gellan powder was dispersed into 100 ml deionized water in a pre-weighed beaker and heated to the boiling point in about 15 min with constant magnetic stirring. The gellan solution was then weighed and hot water was added to compensate for the water loss during heating. Simultaneously, a predetermined amount of calcium chloride dehydrate crystals (ACS reagent, Mallinckrodt Baker, Inc., Phillipsburg, NJ, USA) was added to prepare gellan dispersion with a selected calcium concentration (0–40 mM). The gellan solution was maintained at a temperature slightly below the boiling point and stirred for two min, and then immediately used for NIR analysis.

The whey protein solution (20% w/w) was prepared at room temperature by dispersing whey protein (20 g) into deionized water (80 g) and blending the mixture with a commercial blender to make a homogeneous dispersion.

2.2. NIR spectral acquisition

A DPA-20 spectrophotometer coupled with a fibre optic probe (DSquared Development Inc., La Grande, OR, USA) was used to acquire NIR spectra in the diffuse reflectance mode. The diameter of the fibre optic probe was about one centimetre. Spectra were recorded from 600 to 1100 nm at 0.5 nm intervals.

A gellan or whey protein dispersion was transferred to a custom-built stainless steel test cell with water jacket surrounding the sample holder of the cell (Fig. 1).

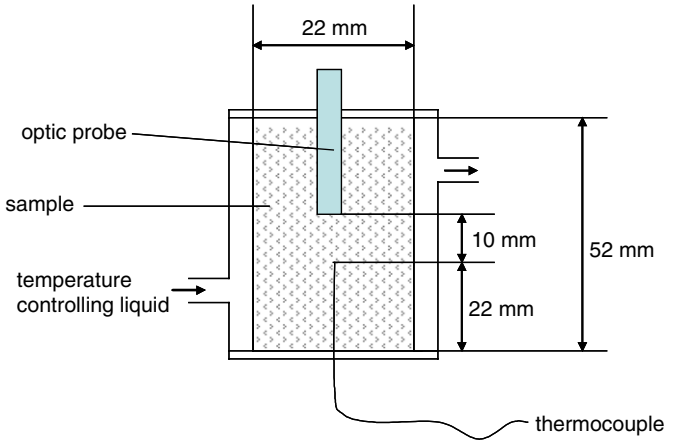

Fig. 1. Schematic representation of positions of fibre-optic probe and thermocouple probe in the test cell for NIR spectral acquisition of a tested hydrocolloid.

The inner diameter of the test cell was 22 mm.The fibre optic probe was immersed into the gel dispersion from the top of the test cell to record NIR spectra. The distance (light path length) between the end of the optic probe and the inner bottom of the test cell was 32 mm. A thermocouple thermometer with the thermocouple probe positioned at the center of the test cell was used to determine the temperatures of gellan or whey protein dispersion. The test cell was sealed and the temperature of the cell was controlled by circulating temperature-controlled liquid (90% v/v ethylene glycol) with a programmable circulator pump through the water jacket of the test cell. Prior to sample spectral collection, a reference spectrum was acquired for the test cell without sample. The reference spectrum was subtracted automatically from each gel spectrum to remove background interference.

A series of NIR spectra corresponding to selected temperatures were recorded continuously for a tested hydrocolloid. Spectra were recorded at about 0.4 °C intervals as the tested dispersion was heated or cooled. For whey protein dispersions, samples were heated from 25 to 95 °C. For gellan dispersions, NIR spectra were recorded by cooling the gellan dispersions from around 95 to 50 °C or from 80 to 30 °C for HA and LA, respectively, and then the sample temperature was raised back to the starting temperature. Duplicate experiments were conducted for each treatment.

2.3. Data analyses

Data analyses were conducted by using DeLight 3.2 software package (DSquared Development Inc., La Grande, OR). Prior to multivariate data analysis, spectra pre-transformations including binning, smoothing, first-order polynomial subtraction or second derivative transformation were conducted to remove baseline shifts, increase the signal to noise ratio, and separate overlapped bands. Principal component analysis (PCA) and principal component regression (PCR) were selected to interpret spectral data.

PCA is a conventional technique to compress a large number (n) of correlated variables (absorbencies at different wavelengths) into a small number (p) of uncorrelated variables defined as principal components (PC), eigenvectors or loadings. The original data set with m spectra and each spectrum composed of n variables can be represented as a matrix $A_{m\times n}$. The original data matrix was decomposed to find the best fit product of scores ($S_{m\times p}$) and linear independent loadings ($L_{p\times n}$) matrices, represented as $A_{m\times n} = S_{m\times p} \times L_{p\times n}$. The first PC accounts for the most amount of variance in data and subsequent PCs account for less and less variance in data. The calculated loadings or PCs are ultimately determined by the constituents of samples, and can be used to predict unknown samples. The scores are unique to each separated PC and each sample spectrum. The scores can be used in place of spectral absorbencies of a sample for data interpretation (Graham, 1993).

In this study, PCA with up to four PCs was used for characterizing gelling agents and determining gelling temperature.

PCR with leave-one-out cross validation was used to investigate the possibility of determining temperatures of gellan dispersions during cooling and heating processes. The performance of PCR models was indicated by R^2 (predicted temperature against the actual temperature), RMS error of predicted temperature, and ratio of performance to deviation (RPD):

$$\mathrm{RMS} = \sqrt{\frac{\sum_{i=1}^{n}(\hat{c}_i - c_i)^2}{n}}. \quad (1)$$

In Eq. (1), $\hat{c}_i$ represents the predicted temperature values by the PCR model, c_i is the actual temperature values, and n is the number of samples.

The RPD is the ratio of the standard deviation of sample temperature values to the standard error of temperature values predicted by the model. The higher RPD value, the better predictability for a PCR model. An RPD of greater than 10 indicates excellent predictability of a model. An RPD of 5–10 is normally acceptable for quality control, and a RPD of 2.5–5 is satisfactory for screening purpose.

3. Results and discussion

3.1. Spectral features as affected by temperature and phase states of hydrocolloids

Fig. 2 presents the second derivative transformation of representative NIR spectra for whey protein (Fig. 2a), LA gellan (Fig. 2b), and HA gellan dispersion (Fig. 2c). There were one major water band discernable at around 970 nm and two weak water bands observable at around 740 and 840 nm for all three hydrocolloids (Huang, Tang, Swanson, Cavinato et al., 2003). The spectra of all three hydrocolloids had prominent NIR spectral features of pure water because of the dominant water content (ca. 99% for gellan

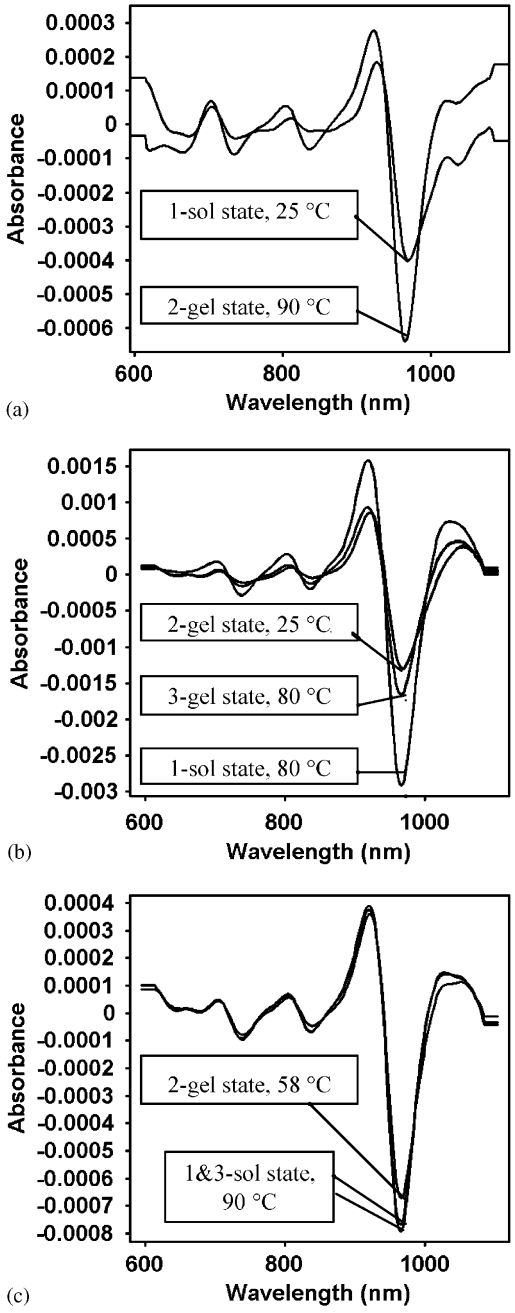

Fig. 2. Representative NIR spectra after second derivative transformation of (a) whey protein, (b) LA gellan, and (c) HA gellan dispersion during heating (for whey protein) or cooling-then-heating (for LA and HA gellan) process. The "gel state" and "sol state" indicated in the figures were visually identified.

and 80% for whey protein) in the dispersion systems. NIR spectra of whey protein exhibited another peak at around 1030 nm, which may be related to the N–H stretching second overtone of protein (Osborne & Fearn, 1986), while both LA and HA gellan spectra exhibited no obvious peaks other than water bands.

The effects of temperatures and/or phase states (sol or gel) on the NIR spectra were quite obvious (Fig. 2). For whey protein dispersions, when the temperature was increased from 25 to 90 °C, protein denaturation led to gel formation, resulting in the shifting of sharp water bands in NIR spectra to lower wavelength (Fig. 2a). Spectral changes of HA gellan dispersions followed a different trend from LA gellan dispersions during the cooling-then-heating cycle. For HA gellan dispersions (Fig. 2c), the initial spectrum (spectrum 1-sol state, 90 °C) was almost completely overlapped with the ending spectrum (spectrum 3-sol state, 90 °C), indicating that the sol–gel transition of HA gellan dispersion was reversible or partially reversible. However, for LA gellan dispersions (Fig. 2b), the initial spectrum (spectrum 1-sol state, 80 °C) and the ending spectrum (spectrum 3-gel state, 80 °C) had different features and could be differentiated indicating the irreversibility of the sol–gel transition of LA gellan dispersions.

Sol–gel transitions of gellan dispersions result from the formation of double helices and subsequent aggregation of these double helices to 3D networks. The absorption intensity in NIR region of a biopolymer dispersion system is affected by light scattering of the system. The intensity of light scattering increases with the increase of crosslinks among macromolecules as well as the formation of junction zones (Mao, Liu, Huglin, & Holmes, 1998; Tang, Mao, Tung, & Swanson, 2001). In Fig. 2b, the spectrum-3 (gel state) exhibited lower absorption rates at the 970 nm water band than the spectrum-1 (sol state), indicating that gellan gel had a higher intensity of light scattering rate than its solution counterpart. This is consistent with the study result of Mao et al. (1998).

PCA results of gellan spectra during the cooling-then-heating process exhibited difference in sol–gel transition between LA and HA gellan dispersions (Fig. 3). For LA gellan, during the cooling process, the plots of PCA scores revealed a U-shape feature, which is mainly related to the change from sol to gel state of gellan dispersion (Huang, Tang, Swanson, Cavinato et al., 2003); after gellan dispersion reached to a completely gel state (such as at 25 °C), when sample was heated up to the starting temperature (80 °C), the plots of PCA scores revealed an almost straight line (likely related to the temperature change) instead of a U-shape feature, which indicated the irreversibility of sol–gel transition of LA gellan dispersion (Fig. 3a). For HA gellan, the shapes of the plots of PCA scores were similar between cooling and heating steps, which indicated the reversibility or at least partial reversibility of sol–gel transition of HA gellan dispersion (Fig. 3b).

3.2. Sol–gel transitions of whey protein, low acyl and high acyl gellan dispersions

PCA with only two PCs could differentiate between sol and gel states for all three tested hydrocolloids during heating or cooling process. The first two PCs of PCA explained about 90–95% of the spectral variance. Similar to the results of our previous study (Huang, Tang, Swanson, Cavinato et al., 2003), the first PC of PCA may be directly related to the sample temperature while the

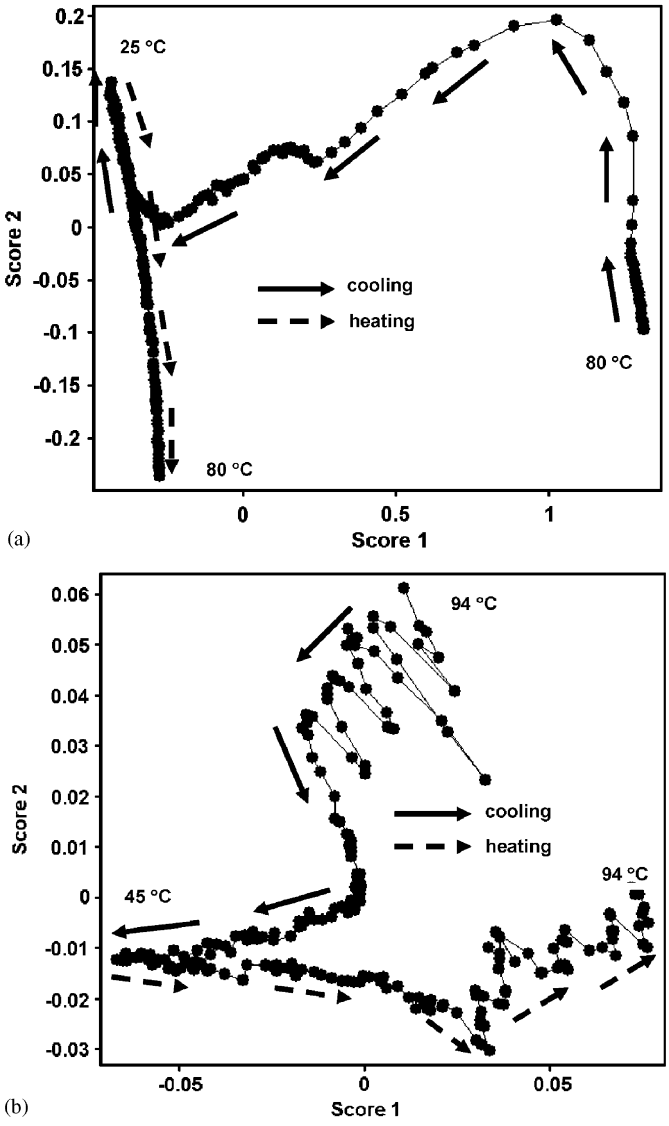

Fig. 3. Plots of the first two scores from PCA of spectral data for (a) LA gellan dispersion during cooling (80–25 °C) and then heating process (25–80 °C), and (b) HA gellan dispersion during cooling (94–45 °C) and then heating process (45–94 °C). The arrows in the figure indicated the sequence of the cooling and heating process.

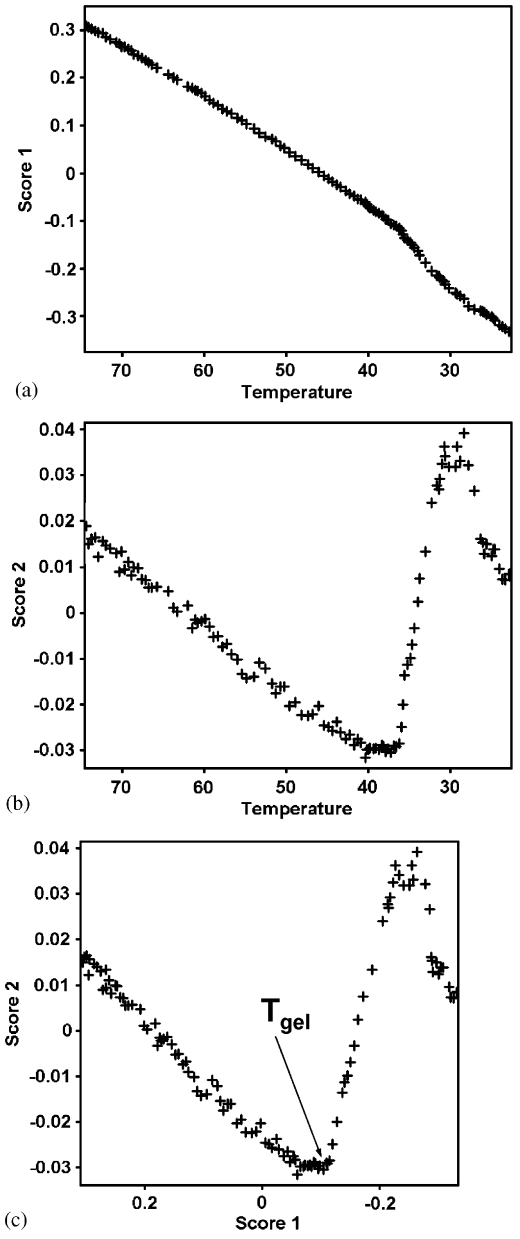

Fig. 4. Plots of the first two scores from PCA of spectral data—(a) score 1 vs. temperature, (b) score 2 vs. temperature, and (c) score 1 vs. score 2, for a 1% LA gelling solution with 4 mM calcium added.

second PC is more likely related to the change in chemical and physical properties during sol–gel transitions (Fig. 4a and b). In this study, the gelling temperature was defined as the turning point of the U-shape on a PCA plot of spectral data collected during the cooling process of gellan, or for whey protein dispersion during the heating process (Fig. 4c). In addition, for reversible HA gellan, the melting temperature (gel–sol transition) was determined through a similar approach.

3.2.1. Whey protein

PCA results exhibited that whey protein dispersions were in a completely sol state at temperatures below 63.4 °C, in a gel state above 75.7 °C and in a sol–gel intermediate state between these two temperatures (Fig. 5). This is consistent with the study of Wang, Wig, Tang, and Hallberg (2003) using dielectric property test for the same whey protein product, in which a sol–gel transition was observed at around 70 °C based upon the sudden change in the sample dielectric constant. However, for the dielectric property test, no data was provided regarding the properties of an intermediate transition state. NIR spectral analysis of whey protein dispersions showed a wide sol–gel intermediate state (63.4–75.7 °C), which would be consistent for a material consisting of various macromolecules, such as α-lactalbumin and β-lactoglobulin with different molecular weights and physico-chemical properties. PCA results revealed abrupt changes in spectral feature at 63.4 and 75.7 °C, which may be related to the denaturation of α-lactalbumin and β-lactoglobulin in whey protein.

The denaturation temperature for α-lactalbumin and β-lactoglobulin is ca. 62 °C and 75 °C, respectively (Bottomley et al., 1990; Damodaran, 1996). The two temperatures (63.4, 75.7 °C) detected by NIR methods were slightly higher than those reported in the literatures, which is likely because that the whey protein sample used in this study was different from that used in other studies. Further study is needed to identify possible structural changes at 70.7 and 72.9 °C as showed in the Fig. 5.

3.2.2. Low acyl gellan

The temperatures of LA gellan dispersions during the cooling could be accurately determined based upon their NIR spectra and PCR model (Table 1). Particularly, for gellan dispersions with relatively low Ca^{2+} added (⩽8 mM), PCR models with only 3 PCs (latent variables) could achieve R^2 (predicted temperature values vs. actual temperature values) of 0.9981–0.9998, RPD of 23.0–74.3 and RMS of 0.2–0.6. For gellan dispersions with higher Ca^{2+} (⩾14 mM), PCR models had somewhat lower predictability (R^2, 0.9176–0.9830; RPD, 3.5–7.7; RMS, 1.5–4.1). These results may be due to the fact that gellan dispersions with high Ca^{2+} content are more complicated systems than those with low Ca^{2+} content. High Ca^{2+} in LA gellan dispersions may cause random coils to form partial double helices by ionic bonding even at a relatively high temperature (Matsukawa, Tang, & Watanabe, 1999). The positions and percentages of partially formed double helices may depend upon the temperature as well as the concentrations of gellan and cation, which increases the structural complexity of the gellan dispersion during the cooling and causes poorer prediction results for temperature.

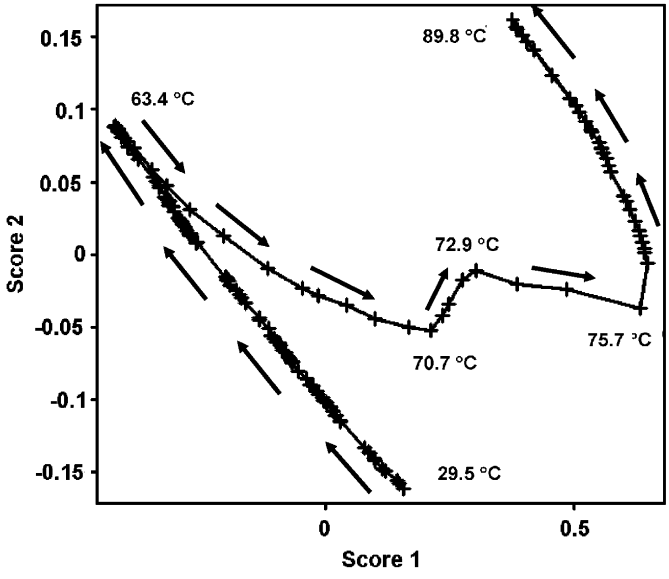

Fig. 5. Plots of score 1 vs. score 2 from PCA of spectral data for a 20% whey protein dispersion heated from 29.5 to 89.8 °C

Sol–gel transition temperatures (Table 2) for LA gellan dispersions determined in this study were close to those determined with dynamic rheological testing reported by Tang et al. (1997) using the same gellan product, indicating the sensitivity of NIR for gelling temperature determination.

PCA results indicate differences in the sol–gel transition between 1% LA gellan dispersions with low Ca^{2+} (⩽8 mM) and with high Ca^{2+} (⩾14 mM) concentrations. LA gellan dispersion with high Ca^{2+} concentration had a smoother sol–gel transition compared to that with lower Ca^{2+} concentration (Figs. 6 and 7). The undergoing mechanism causing this difference is unclear, but should be related to the effect of Ca^{2+} concentration on various interactions between and/or among gellan molecules and water, including the effect on the formation of double helices and the aggregation of these double helices. Various studies pointed out the difference in textural properties between gellan gels with low Ca^{2+} and high Ca^{2+} content (Tang et al., 1996, 1997), which reflects their difference in sol–gel transition mechanisms. A relatively high Ca^{2+} content in LA gellan dispersions may cause partial random coils to form double helices by ionic bonding even at a relatively high temperature (Matsukawa et al., 1999). The percentages of partially formed double helices may increase with the decrease of temperature, and therefore the sol–gel transition of gellan with high Ca^{2+} is a smoothly

Table 1
Statistical results for predicting temperatures of LA gellan dispersions with selected calcium concentrations (2–40 mM) during cooling process by PCR with leave-one-out cross validation

Calcium (mM)	1 PC[a]			2 PCs			3 PCs			4 PCs		
	R^2	RMS	RPD	R^2	RMS	RPD	R^2	RMS	RPD	R^2	RMS	RPD
2	0.9902	1.6	10.1	0.9992	0.5	34.7	0.9998	0.2	74.3	0.9998	0.2	78.6
4	0.9726	2.3	6.0	0.9863	1.6	8.5	0.9993	0.4	37.8	0.9993	0.4	37.8
6	0.9259	3.7	3.7	0.9931	1.1	12	0.9987	0.5	28.1	0.9989	0.5	30.0
8	0.8881	4.4	3.0	0.9344	3.4	3.9	0.9981	0.6	23.0	0.9982	0.6	23.7
14	0.8639	5.2	2.7	0.8737	5.0	2.8	0.9590	2.8	4.9	0.9584	2.9	4.9
30	0.4179	10.9	1.3	0.8840	4.8	2.9	0.9176	4.1	3.5	0.9912	1.3	10.7
40	0.8477	4.6	2.6	0.8474	4.6	2.6	0.9830	1.5	7.7	0.9883	1.3	9.3

[a]Number of principal components used for PCR.

Table 2
Gelling temperature of 1% gellan dispersions determined by NIR and other methods

Gellan dispersion	Added Ca^{++} (mM)								
	0	2	4	6	8	14	15	30	40
LA	—	36.8[a]	41.3	44.6	48.4	51.8	—	66.2	67.0
	—	(35.0)[b]	(40.0)	(44.0)	(46.5)	(53.5)	—	(64.0)	(65.5)
HA	70.2[a]	—	75.1	—	77.3	—	78.5	81.3	—
	(69.5)[c]	—	(73.3)	—	(75.1)	—	(76.6)	(78.2)	—
	(72.4)[d]		(76.2)		(78.8)		(79.9)	(81.2)	

[a]Standard deviation was from 0.04 to 1.84 °C for gelling temperature determined with NIR method.
[b]Data from Tang, Tung, and Zeng (1997) with dynamic rheological testing method for gelling temperature determination.
[c]Data from Huang, Singh, Tang, and Swanson (2004) with dynamic rheological testing method for gelling temperature determination.
[d]Gel–sol (melting) transition temperature determined with NIR method.

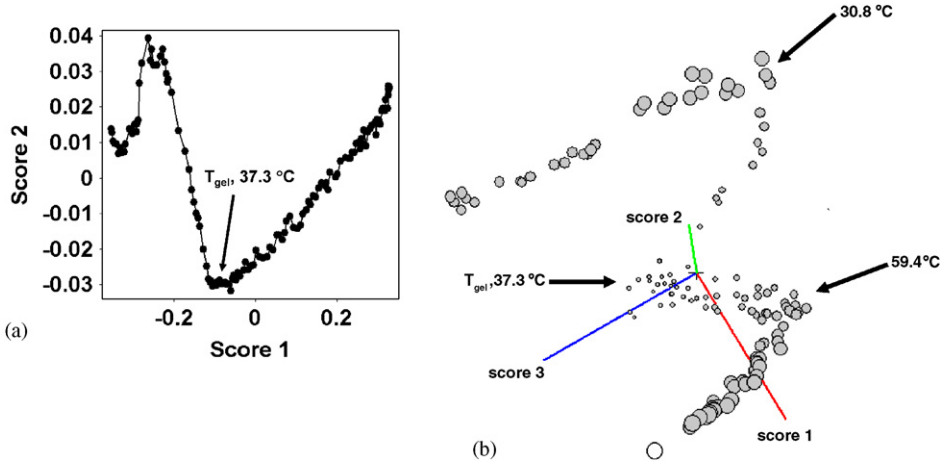

Fig. 6. Plots of the first three scores from PCA for a 1% LA gellan dispersion with 2 mM Ca^{2+} added that was cooled from 76 to 21 °C: (a) score 1 vs. score 2; (b) 3D image of the first three scores which was adjusted at an angle that clearly showed two transitions at around 30.8 and 59.4 °C.

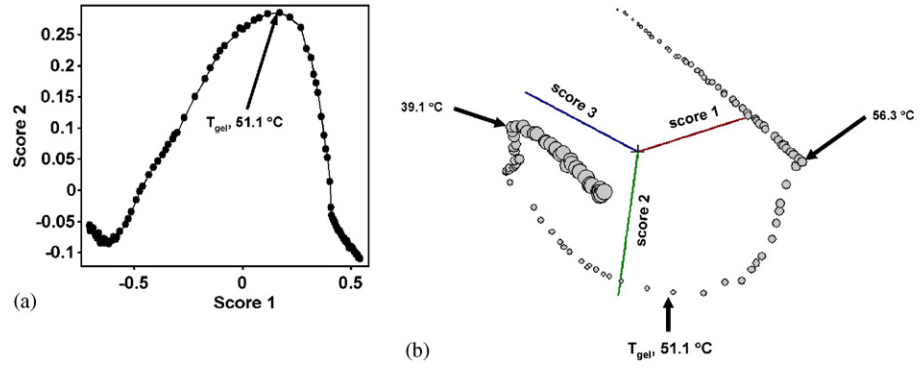

Fig. 7. Plots of the first three scores from PCA for a 1% LA gellan dispersions with 14 mM Ca^{2+} added that was cooled from 75 to 26 °C: (a) score 1 vs. score 2; (b) 3D image of the first three scores which was adjusted at an angle that clearly showed two transitions at around 39.1 and 56.3 °C.

continuous procedure at a relatively wide temperature range.

In addition to providing information on sol–gel transitions of LA gellan dispersions, the NIR method may be able to discern other property changes of LA gellan dispersions, such as at around 30.8 and 59.4 °C for LA gellan dispersion with 2 mM Ca^{2+} added, and at 39.1 and 56.3 °C for LA gellan dispersions with 14 mM Ca^{2+} added (Fig. 6 and 7). These spectral changes may be related to the initial transition of random coil-double helix and complete aggregation of double helices, which needs further investigation.

Table 3
Statistical results for predicting temperatures of HA gellan dispersions with selected calcium concentrations (0–30 mM) during cooling-then-heating process by PCR with leave-one-out cross validation

Calcium (mM)	1 PC[a]			2 PCs			3 PCs			4 PCs		
	R^2	RMS	RPD	R^2	RMS	RPD	R^2	RMS	RPD	R^2	RMS	RPD
0	0.6883	7.5	1.8	0.9970	0.7	18.4	0.9970	0.7	18.3	0.9977	0.6	20.8
4	0.7807	5.7	2.1	0.9950	0.9	14.1	0.9960	0.8	15.7	0.9980	0.5	22.5
8	0.6613	6.6	1.7	0.9914	1.1	10.8	0.9929	1.0	11.9	0.9969	0.6	18.0
15	0.9686	2.4	5.6	0.9988	0.5	29.3	0.9988	0.5	29.2	0.9990	0.4	31.5
30	0.8768	3.7	2.8	0.9961	0.7	16.1	0.9961	0.7	16.0	0.9972	0.6	18.8

[a]Number of principal components used for PCR.

3.2.3. *High acyl gellan*

Table 3 summarizes PCR results in determining the temperatures of HA gellan dispersions during cooling-then-heating cycles. PCR models with only two PCs could accurately predict temperatures of HA gellan dispersions during the cooling-then-heating cycles (R^2, 0.9914–0.9988; RMS, 0.5–1.1; RPD, 10.8–29.3). PCR models for temperature determinations of 1% HA gellan dispersion showed more consistent results than that for 1% LA gellan dispersions over a similar range of calcium concentrations. This may be because that the HA gellan solution is a more consistent system that is less affected by the calcium compared to its LA gellan counterpart, which is similar to the effect of calcium on gellan gel system. Some studies indicated that HA gellan gels were more stable and less affected by calcium compared to LA gellan counterparts (Huang, Tang, Swanson, & Rasco, 2003; Morris, Gothard, Hember, Manning, & Robinson, 1996).

Gelling temperatures of HA gellan dispersions determined with NIR method (Table 2) were similar to the results of our previous study (Huang, Singh, Tang, & Swanson, 2004). Both studies showed that gelling temperature increased with the increase of calcium content in the HA gellan dispersion, although the gelling temperatures determined with the NIR method were slightly higher than that determined with the dynamic rheological testing method. The gelling temperatures of HA gellan dispersions were less affected by calcium compared to similar LA gellan dispersions (Table 2).

PCA results indicate that HA gellan dispersion systems were unstable at relatively high temperatures or in sol state (Fig. 3b). One possible explanation is that part of random coils formed double helices and these double helices may even partially aggregate through hydrogen bonds and ionic bonds between Ca^{2+} and the carboxylate groups of gellan molecules at high temperatures. However, formation of these double helices or other association of molecules may just be temporary, followed by rapid dissociation and then new association of molecules, which eventually makes the whole gellan dispersion system unstable at relatively high temperature.

The similarity of spectral features between the cooling and the heating processes indicates the reversibility of sol–gel transition of HA gellan (Fig. 3b). The difference of spectral features between the cooling and the heating processes may be due to the time dependant and aging effects on structural properties of the HA gellan dispersion (Takigawa, Nakajima, & Masuda, 1999). Accordingly, the corresponding gel–sol transition temperatures (T_{melt}) were slightly different from the gelling temperature (Table 2).

4. Conclusion

NIR method can be a potential tool for monitoring sol–gel transitions of food hydrocolloids including whey protein, LA, and HA gellan gum as well as other food hydrocolloids. NIR method revealed that sol–gel transitions of LA gellan dispersions were not reversible while that of HA gellan dispersions were partially reversible in which a time-dependant factor playing an important role.

NIR is a reliable method for predicting gelling temperatures during sol–gel transitions and may be used to determine empirical changes in the structures of protein and carbohydrate gelling agents during heating or cooling processes. Unlike commonly used NIR techniques for quantitative analysis that required reference values for the development of a chemometric model, in this study the gelling temperature were determined directly based upon the PCA results in the absence of reference values.

NIR method confirmed that a change in calcium concentration affects the sol–gel transition mechanisms of gellan dispersions, although we cannot draw a conclusion about sol–gel transition mechanism of gellan or whey protein from the results of this study.

Accuracy of the NIR method may be affected by the temperature variance of a selected hydrocolloid in the test cell (Fig. 1). A smaller test cell would be more effective for temperature control in the future study. In addition, an extended wavelength range (700–2500 nm) could provide more information on molecular structure that enable for a better understanding of the sol–gel transition mechanisms of biopolymers.

Interpretation of NIR spectra could be difficult, which requires a deep understanding of the tested sample. This study was possible because of our previous research experience in NIR method and first hand data on

physico-chemical properties of gellan gums. There is still a long way to go to fully apply NIR method in characterization of food hydrocolloid systems. However, NIR method could be a powerful tool for characterization of food hydrocolloids, since it can non-destructively monitor the change in molecular structures involving functional groups containing hydrogen-stretching vibration (O–H, C–H and N–H), particularly for the change of water bands. Furthermore, development of instrument and computer technology increases the sensitivity of NIR instrument, lowers the instrumental cost and makes it easy to operate.

Acknowledgements

This research was sponsored in part by the United States Department of Agriculture National Research Competitive Grants programs (NRI-2001-35503-10770 and NRI-2001-35503-10033), and the City University of New York (PSC-CUNY #60122-3536). We thank CP Kelco Inc. for providing gellan gum, and NZMP Inc. for providing whey protein. Special thank goes to Dr. David M. Mayes, DSquared Development, Inc. for his assistance with the data analysis.

References

Bao, J. S., Cai, Y. Z., & Corke, H. (2001). Prediction of rice starch quality parameters by near infrared reflectance spectroscopy. *Journal of Food Science*, *66*, 936–939.

Bottomley, R. C., Evans, M. T. A., & Parkinson, C. J. (1990). Whey proteins. In P. Harris (Ed.), *Food gels* (pp. 435–466). London, England: Elsevier.

Castillo, M. Z., Payne, F. A., Hicks, C. L., Laencina, J. S., & Lopéz, M.-B. (2003). Modelling casein aggregation and curd firming in goats' milk from backscatter of infrared light. *The Journal of Dairy Research*, *70*, 335–348.

Closs, C. B., Conde-Petit, B., Roberts, I. D., Tolstoguzov, V. B., & Escher, F. (1999). Phase separation and rheology of aqueous starch/galactomannan systems. *Carbohydrate Polymers*, *39*, 67–77.

Damodaran, S. (1996). Amino acids, peptides and proteins. In O. R. Fennema (Ed.), *Food chemistry* (pp. 356–365). New York: Marcel Dekker.

Graham, R. C. (1993). *Data analysis for the chemical sciences, a guide to statistical techniques*. New York: VCH.

Huang, Y., Singh, P. P., Tang, J., & Swanson, B. G. (2004). Gelling temperature of high acyl gellan as affected by mono- and di- valent cations with dynamic rheological analysis. *Carbohydrate Polymers*, *54*, 27–33.

Huang, Y., Tang, J., Swanson, B. G., Cavinato, A., Lin, M., & Rasco, B. A. (2003). Near infrared spectroscopy: A new tool for studying physical and chemical properties of polysaccharide gels. *Carbohydrate Polymers*, *53*, 281–288.

Huang, Y., Tang, J., Swanson, B. G., & Rasco, B. A. (2003). Effects of calcium concentration on textural properties of high and low acyl mixed gellan gels. *Carbohydrate Polymers*, *54*, 517–522.

Lundin, L., Stenlöf, B., & Hermansson, A.-M. (1998). NIR spectra in relation to viscoelastic properties of mixtures of Na-κ-carrageenan, locust bean gum and casein. *Food Hydrocolloids*, *12*, 189–193.

Mao, R., Liu, Y., Huglin, M. B., & Holmes, P. A. (1998). Dynamic light scattering from polymer gels: Spring-rotor model. *Polymer International*, *45*, 321–326.

Matsukawa, S., Tang, Z., & Watanabe, T. (1999). Hydrogen-bonding behaviour of gellan in solution during structural change observed by ^{1}H NMR and circular dichroism methods. *Progress in Colloid and Polymers Science*, *114*, 15–24.

Morris, E. R., Gothard, M. G. E., Hember, M. W. N., Manning, C. E., & Robinson, G. (1996). Conformational and rheological transitions of welan, rhamsan and acylated gellan. *Carbohydrate Polymers*, *30*, 165–175.

Osborne, B. G., & Fearn, T. (1986). *Near infrared spectroscopy in food analysis*. New York: Wiley.

Segtnan, V. H., Kvaal, K., Rukke, E. O., Schüller, R. B., & Isaksson, T. (2003). Rapid assessment of physico-chemical properties of gelatine using near infrared spectroscopy. *Food Hydrocolloids*, *17*, 585–592.

Takigawa, T., Nakajima, K., & Masuda, T. (1999). Rheological properties of the gellan/water system. *Progress in Colloid and Polymers Science*, *114*, 62–67.

Tang, J., Mao, R., Tung, M. A., & Swanson, B. G. (2001). Gelling temperature, gel clarity and texture of gellan gels containing fructose or sucrose. *Carbohydrate Polymers*, *44*, 197–209.

Tang, J., Tung, M. A., & Zeng, Y. (1996). Compression strength and deformation of gellan gels formed with mono- and divalent cations. *Carbohydrate Polymers*, *29*, 11–16.

Tang, J., Tung, M. A., & Zeng, Y. (1997). Gelling temperature of gellan solutions containing calcium ions. *Journal of Food Science*, *62*, 276–280.

Thygesen, L. G., Engelsen, S. B., Madsen, M. H., & Sorensen, O. B. (2001). NIR spectroscopy and partial least squares regression for the determination of phosphate content and viscosity behaviour of potato starch. *Journal of Near Infrared Spectroscopy*, *9*, 133–139.

Wang, Y., Wig, T. D., Tang, J., & Hallberg, L. M. (2003). Dielectric properties of foods relevant to RF and microwave pasteurization and sterilization. *Journal of Food Engineering*, *57*, 257–268.